PHYSICAL REVIEW D VOLUME 25, NUMBER 1 1 JANUARY 1982

Quark sea in nuclei and its effects in Drell-Yan processes

R. M. Godbole and K. V. L. Sarma
Tata Institute of Fundamental Research, Homi Bhabha Road, Bombay 400005, India
(Received 13 November 1980)

The sea of quark-antiquark pairs arising from the interactions between the nucleons within the target nucleus leads to important consequences in a hard-scattering process. We have investigated the implications of such a quark sea for inclusive reactions involving massive dimuons initiated by hadrons off nuclei, assuming the validity of the Drell-Yan model. Besides the dependence on the variables x_F and (m^2/s), the exponent α is expected to depend on the beam type and also on the specific nuclei used as targets.

I. INTRODUCTION

The production of lepton pairs in hadron collisions has been a field of great interest in recent years. Several features of the experimental data on massive-lepton-pair production have been described[1] on the basis of the Drell-Yan mechanism[2] in which a virtual photon produced by the annihilation of a quark-antiquark system gives rise to the observed lepton pair. As most of these experiments utilize nuclear targets having large values of mass number A, the "per nucleon" cross section has been extracted by dividing the observed cross section by A^α, where the value of α has been invariably taken to be unity. Clearly a small uncertainty in α can result in a sizable uncertainty in the overall normalization of the cross section. Furthermore, a knowledge of the correct A dependence is also crucial for the proper determination of the so-called K factor,[3] which is the ratio of the measured cross section on a nucleon target to the one predicted by the Drell-Yan model without taking into account the corrections arising from quantum chromodynamics (QCD).

The available experimental information on the A dependence is not extensive and somewhat confusing. The results of the pA scattering experiments of the Columbia–Fermilab–Stony Brook (CFS) group[4] and also the $\pi^\pm A$ experiments of the CERN NA-3 group[3,5] are consistent with the value $\alpha = 1$, whereas the data of the Chicago-Illinois-Princeton (CIP) group[6] with the 225-GeV/c π^- beam have given $\alpha = 1.12 \pm 0.05$. It has been pointed out recently that this apparent discrepancy might be due to the fact that these groups are measuring the A dependence of different observables.[7]

In the customary description of the hard-scattering processes the nucleus is viewed as a collection of slowly moving nucleons weakly bound to each other, and to each nucleon one associates three valence quarks and an intrinsic $q\bar{q}$ sea. For a target nucleus A the cross section is taken to be the mass number A times the contribution coming from a single nucleon N. However, this may be an underestimate of the A dependence. As emphasized by Krzywicki,[8] due to the smallness of time scales and distance scales involved in the hard-scattering processes, it does not make sense to employ the customary time-averaged description of the nucleus. One should rather adopt a picture of the nucleus which includes an additional nuclear sea arising due to the mutual interactions between the nucleons of the nucleus. Thus in any hard-scattering process one should allow for the possibility that the exchange of mesons, or equivalently $q\bar{q}$ pairs, is taking place between the bound nucleons, and hence the total quark sea in the nucleus is more than a mere sum of intrinsic seas of the individual nucleons. From this viewpoint it is therefore natural to expect

$$\sigma(bA \to \mu^+\mu^- + \cdots) > A\sigma(bp \to \mu^+\mu^- + \cdots),$$

where b denotes the hadron in the incident beam, i.e., the value of the parameter $\alpha > 1$.

The presence of an additional quark sea in nuclei is perhaps also hinted at by the experimental observation[9] of large rates for finding a hadron at large values of transverse momenta p_T in hadron-nucleus collisions. Here the measured rates are larger than what are predicted by a naive linear A extrapolation of the rates corresponding to a proton target. An even more prominent nuclear enhancement has been observed in the production of jets of hadrons at large values of p_T, with both proton and pion beams on hydrogen and aluminum targets.[10] There have been some attempts to understand these large rates with nuclear targets by invoking multiple scattering of partons,[11] and also by assuming the production of multiquark jets.[12] However, a natural explanation for this phenomenon might be provided if one adopted the viewpoint originally advocated by Krzywicki.[8] According to this if one assumes an increased nuclear sea, then due to the availability of many more partons in the target one may be able to understand the anomalous nuclear enhancement in the production of single hadrons as well as jets at high p_T. Although this hope is yet to be borne

out by detailed calculations, at least in regard to jets, it seems worthwhile examining the experimental consequences of an increased quark sea in nuclei, first in the simple case of Drell-Yan processes wherein the quark fragmentation functions, etc., do not appear.

In Sec. II we incorporate the contributions of the additional quark-antiquark sea in nuclei to the Drell-Yan processes, and estimate the parameters that characterize it with the help of the available data on dimuon production. In Sec. III we discuss in detail the observable consequences of the proposed nuclear sea: the sensitivity of the A dependence to the projectile, to the incident energy, and also to the specific target nuclei employed in the experiments. Section IV is devoted to a brief survey of our results and some concluding remarks.

II. FORMALISM

If b denotes the hadron in the beam and A denotes the target nucleus, the cross section for the process

$$bA \to \mu^+\mu^- + \text{hadrons},$$

according to the classical Drell-Yan model, is

$$\frac{d^2\sigma^{bA}}{dx_F dm^2} = \frac{1}{s x_F}\frac{x_1 - x_2}{x_1 + x_2}\frac{d^2\sigma^{bA}}{dx_1 dx_2}, \tag{1}$$

where

$$\frac{d^2\sigma^{bA}}{dx_1 dx_2} = K\frac{4\pi\alpha^2}{9 s x_1^2 x_2^2} H^{bA}(x_1, x_2) \tag{2}$$

and

$$H^{bA}(x_1, x_2) \equiv \sum_f Q_f^2 [\bar{f}^b(x_1) f^A(x_2) + f^b(x_1)\bar{f}^A(x_2)]. \tag{3}$$

Here $\sqrt{s}$ is the total energy in the center-of-mass system of b and a nucleon of the target A, and x_1 and x_2 are the Bjorken variables of the participating partons. The mass m and the Feynman variable x_F of the muon pair are given by the relations

$$m^2 = x_1 x_2 s, \tag{4}$$

$$x_F = \frac{q_L^{\text{c.m.}}}{q_{\max}^{\text{c.m.}}} \tag{5}$$

$$\simeq \frac{x_1 - x_2}{1 - (m^2/s)}. \tag{6}$$

The factor K is an overall normalization factor which equals unity in the Drell-Yan model, while its experimental value[3] with proton target is $K \sim 2$. The K factor in any case is not expected to depend on the mass number of the target nucleus and hence for the determination of the α in the A dependence, [where only the ratios of cross sections are to be used as in Eqs. (13)–(15)] the exact value of K is irrelevant.

The quark of flavor f and electric charge $(4\pi\alpha)^{1/2}Q_f$ has the distribution function $f^h(x)$, which is so normalized that $(1/x)f^h(x)$ is the probability for the quark to have a longitudinal momentum fraction x in the hadron h. Writing $f(x)$ as a sum of the valence and sea components,

$$f(x) = f_v(x) + f_s(x), \tag{7}$$

and using the relation

$$f_s(x) = \bar{f}_s(x) \tag{8}$$

in Eq. (3), we have

$$H^{bA}(x_1, x_2) = \sum_f Q_f^2 \{[\bar{f}_v^b(x_1) + f_s^b(x_1)] f_v^A(x_2) + [\bar{f}_v^b(x_1) + f_v^b(x_1) + 2f_s^b(x_1)] f_s^A(x_2)\}. \tag{9}$$

A. Inclusion of quark sea in nuclei

The hypothesis of an enhanced $q\bar{q}$ sea in the target nucleus A shall be incorporated by expressing the valence and sea quark distributions for a nucleus of mass number A and charge number Z as follows:

$$f_v^A(x) \equiv A f_v^N(x) = A\left(\frac{Z}{A} f_v^p(x) + \frac{A - Z}{A} f_v^n(x)\right), \tag{10}$$

$$f_s^A(x) = A f_s^N(x) + \tfrac{1}{2}A(A-1)\delta(1-x)^\mu. \tag{11}$$

In the last equation the function $f_s^N(x)$ refers to the intrinsic sea associated with a free nucleon N (as extracted, for instance, from deep-inelastic lepton scattering on hydrogen), and the second term is motivated by the exchange of $q\bar{q}$ pairs between the $A(A-1)/2$ pairs of nucleons in the nucleus. The assumption here is that during the very short time implied by the hard scattering process one should take into account the total quark-antiquark sea arising both from vacuum fluctuations and mutual interactions between all the bound nucleons. The two parameters δ and μ control the "strength" and "hardness" of the proposed additional nuclear sea, which shall be taken for simplicity to be SU(3) symmetric.

The expression for $H^{bA}(x_1, x_2)$ thus becomes

$$H^{bA}(x_1, x_2) = A \sum_f Q_f^2 \{[\bar{f}_v^b(x_1) + f_s^b(x_1)] f_v^N(x_2) + [\bar{f}_v^b(x_1) + f_v^b(x_1) + 2f_s^b(x_1)] f_s^N(x_2)$$

$$+ \tfrac{1}{2}(A-1)[\bar{f}_v^b(x_1) + f_v^b(x_1) + 2f_s^b(x_1)]\,\delta(1-x_2)^{\mu}\} . \tag{12}$$

For example, in the case of a $\bar{p}$ beam the first term in Eq. (12) dominates over all the other terms, whereas for a proton beam, due to the absence of a valence antiquark, it is possible for the term proportional to $(A-1)$ in H^{bA} to gain in relative importance in certain kinematic regions.

Substituting Eq. (12) in Eq. (2) and numerically integrating Eq. (1) over x_F and/or m in the ranges appropriate for the experimental data, we can obtain the cross sections σ^{bA}, $d\sigma^{bA}/dx_F$, and $d\sigma^{bA}/dm$. For a given incident momentum of the beam b, producing dimuons in identical kinematical ranges but from targets of different mass numbers, say A_1 and A_2, we define the quantities of experimental interest, α^b, $\alpha^b(x_F)$, and $\alpha^b(m)$, by the following ratios:

$$\frac{\sigma^{bA_1}}{\sigma^{bA_2}} = \left(\frac{A_1}{A_2}\right)^{\alpha^b} , \tag{13}$$

$$\frac{d\sigma^{bA_1}/dx_F}{d\sigma^{bA_2}/dx_F} = \left(\frac{A_1}{A_2}\right)^{\alpha^b(x_F)} , \tag{14}$$

$$\frac{d\sigma^{bA_1}/dm}{d\sigma^{bA_2}/dm} = \left(\frac{A_1}{A_2}\right)^{\alpha^b(m)} . \tag{15}$$

It should be noted that these definitions of the α's depend not only on the mass numbers A_1 and A_2 but also, as will become clear in Sec. III C, on the differences in the (Z/A) ratios in different targets through Eq. (10). Moreover, due to the accessibility of varied and restricted kinematic regions in the experiments, the values of α depend implicitly on the ranges of integration; for example, in expression (15)

$$\left(\frac{A_1}{A_2}\right)^{\alpha^b(m)} = \left(\int_{x_{F1}}^{x_{F2}} (d^2\sigma^{bA_1}/dm\,dx_F)dx_F\right) \Big/ \left(\int_{x_{F1}}^{x_{F2}} (d^2\sigma^{bA_2}/dm\,dx_F)dx_F\right) , \tag{16}$$

the function $\alpha^b(m)$ depends on the range of integration $x_{F1} \leq x_F \leq x_{F2}$. In addition, a possible dependence of the α's on the variable s is understood, as will become clear later. While one can also define a function $\alpha(q_T)$, we shall not however consider it here because the transverse momentum q_T of the dimuon is believed to arise from QCD corrections and from the primordial momenta associated with the participating partons, which ought to be only corrections to the simple Drell-Yan model.

B. Input structure functions

We have calculated the values of α defined through Eqs. (13)–(15) for the CIP data[6] of the 225-GeV/c π^- beam on a copper target ($A_1 = 64$) and a tungsten target ($A_2 = 184$) for the production of dimuons in the ranges $4 \leq m \leq 8.75$ GeV and $0 \leq x_F \leq 1$. For the proton beam data at 400 GeV/c on Be and Pt targets and $5 \leq m \leq 15$ GeV, while obtaining $d\sigma/dm$ we have integrated over the x_F range $-0.15 \leq x_F \leq 0.075$, which corresponds to the acceptance in the experiment of the CFS group.[4]

The nucleon structure functions have been taken from the analysis of the CERN-Dortmund-Heidelberg-Saclay (CDHS) data,[13] wherein the intrinsic sea of the nucleon N is taken to be SU(3) nonsymmetric. These functions of the CDHS group as listed in Ref. 3 are

$$u_v^p(x) = 2.2x^{0.51}(1-x)^{2.8} \tag{17}$$

$$d_v^p(x) = 1.25x^{0.51}(1-x)^{3.8} \tag{18}$$

$$S^N(x) \equiv u_s^N(x) = d_s^N(x) = 2s_s^N(x) = 0.27(1-x)^{8.1} . \tag{19}$$

We have also repeated the calculations with the nucleon structure functions determined from the dimuon production data of the NA3 group[3]:

$$u_v^p(x) = 2.24x^{0.5}(1-x)^{3.2} , \tag{20}$$

$$d_v^p(x) = 1.25x^{0.5}(1-x)^{4.2} , \tag{21}$$

$$u_s^N(x) = d_s^N(x) = 2s_s^N(x) = 0.37(1-x)^{9.4} . \tag{22}$$

In both the calculations (using either of the above two sets of functions), the pion structure was taken to be the one given by the analysis of the 200-GeV/c data of the NA3 group[3] with the SU(3)-symmetric sea:

$$V^{\pi}(x) \equiv \bar{u}_v^{\pi^-}(x) = d_v^{\pi^-}(x) = 0.55x^{0.4}(1-x)^{0.9} , \tag{23}$$

$$S^{\pi}(x) \equiv u_s^{\pi^-}(x) = 0.09(1-x)^{4.4} . \tag{24}$$

In choosing the values of the two parameters δ and μ in Eq. (12), it was required that we obtain an overall agreement with the available data on $\alpha^{\pi^-}(x_F)$ of the CIP group and $\alpha^p(x_F)$ of the CFS group. Table I shows that the calculated values of α defined in Eq. (13) do not depend on which set of the nucleon structure functions is used; they are also insensitive to the precise values of the two parameters δ and μ provided they are taken around the values,

$$\delta = 3.5 \times 10^{-3} , \tag{25}$$

$$\mu = 15 . \tag{26}$$

The determination of these parameters is insensitive to the presence or absence of the pion sea given in Eq. (24). We shall therefore regard the above values as typical values for the purposes of estimating the effects of the additional nuclear sea defined in Eq. (11)[14]; in our later calculations we shall only use the values in Eqs. (25) and (26) together with the CDHS nucleon functions (17)–(19) and the pion structure functions (23) and (24).

III. IMPLICATIONS ON A DEPENDENCE

We shall preface this section with a few general comments to make some of the salient features emerging from our calculations plausible. From Eqs. (4) and (6), setting $1 - m^2/s \simeq 1$, the annihilating parton in the target nucleon has the longitudinal momentum fraction

$$x_2 = \tfrac{1}{2}[(x_F^2 + 4m^2/s)^{1/2} - x_F] . \tag{27}$$

Of special interest are the following limiting behaviors at small and large values of x_F:

$$\text{at small } |x_F| \ (|x_F| \ll 2m/\sqrt{s}): \quad x_2 \simeq \frac{m}{\sqrt{s}} - \frac{1}{2}x_F , \tag{28}$$

$$\text{at large } x_F \ (x_F \gg 2m/\sqrt{s}): \quad x_2 \simeq (m/\sqrt{s})^2 \frac{1}{x_F} . \tag{29}$$

Due to the sharp $(1/m^3)$ decrease of the Drell-Yan cross section the average value of m will be closer to the lower limit on m, which is generally taken to be around 4–5 GeV. For the Fermilab and CERN SPS experiments therefore, the quantity $(2m/\sqrt{s}) \simeq 0.4$.

According to Eqs. (11), (25), and (26) the additional quark-sea *per nucleon* in the nucleus of mass number A is

$$S_a^N(x_2) = \frac{(A-1)}{2} 3.5 \times 10^{-3} (1 - x_2)^{15} , \tag{30}$$

which is very much concentrated near $x_2 = 0$ with an average $\langle x_2 \rangle \simeq 0.06$. We therefore expect the additional sea to enhance the dimuon production (by virtue of Eq. 29), particularly at large x_F and at small values of m; i.e., $\alpha(x_F)$ should increase[15] with x_F, while $\alpha(m)$ should decrease with m at a fixed $\sqrt{s}$. Measurements at small *negative* values of x_F (data of CFS group), on the other hand, imply x_2 values which, due to Eq. (28), will not be small enough to clearly reveal the effects of the additional nuclear sea.

As we go to higher energies the influence of the additional sea at large x_F (and fixed m) should be more marked, because $x_2 \to 0$ faster as $(1/\sqrt{s})^2$ in Eq. (29). It should, however, be recognized that the variation of α with m and s are not independent; since the Drell-Yan formula for $(m^3 d\sigma/dm)$ depends only on the scaling variable $\tau = (m^2/s)$, the resulting A dependence must also scale,

$$\alpha(m, s) = \alpha(m^2/s) .$$

Thus if $\alpha(m, s)$ decreases with m, at a fixed s,

TABLE I. Values of α^b of Eq. (13) calculated with two sets of nucleon structure functions and several values of the sea parameters δ and μ for the experimental conditions of the CIP and CFS groups. The last column, however, refers to the integration range $x_F = 0$–1 and is given for the sake of comparison.

Nucleon structure	μ	$10^3\delta$	α^{π^-} (225 GeV/c) $x_F \geq 0$	α^p (400 GeV/c) $-0.15 \leq x_F \leq 0.075$	$x_F \geq 0$
CDHS	14	3.2	1.04	1.04	1.11
[Eqs. (17)–(19)]	15	3.5	1.04	1.03	1.11
	17	4.0	1.04	1.02	1.11
NA3	13	3.0	1.05	1.06	1.11
[Eqs. (20)–(22)]	14	3.5	1.05	1.05	1.11
	15	4.0	1.05	1.05	1.11

then it should correspondingly increase with s, at a fixed m. These features will become apparent in the results of our calculations presented in the following subsections.

A. Beam dependence of α

The dependence of the functions α^b defined by Eqs. (13)-(15) on the beam mainly stems from the presence or absence of a valence antiquark in the beam hadron b. For instance, the valence $\bar{q}$ in the $\bar{p}$ and K^- beams allows the Drell-Yan mechanism to proceed dominantly through the valence-valence annihilation and thus $\alpha^{\bar{p}}$ and α^{K^-} will be closer to unity, in contrast to α^p and α^{K^+}.

1. π^- beams

In Fig. 1(a) we have plotted the data of the CIP group[6] on $\alpha^{\pi^-}(x_F)$ obtained with the 225 GeV/c π^- beam, together with the curve (solid line) calculated as explained in Sec. II. It is apparent that an increasing trend of $\alpha(x_F)$ is quite consistent with the data. A related consequence of our hypothesis is the prediction of a decreasing $\alpha(m)$ as shown in Fig. 1(b) by the solid curve. As m increases $\alpha(m)$ approaches the curve meant for $\delta=0$, i.e., the case when additional nuclear sea is absent. The fact that this limiting value of $\alpha(m)$ falls below $\alpha=1$ is due to the neutron excess in the target, as will be explained later. The experimental point around $m=7$ GeV in Fig. 1(b) lies about two standard deviations above our expectations. More precise data at more values of m are clearly needed to verify this decreasing trend of $\alpha(m)$.

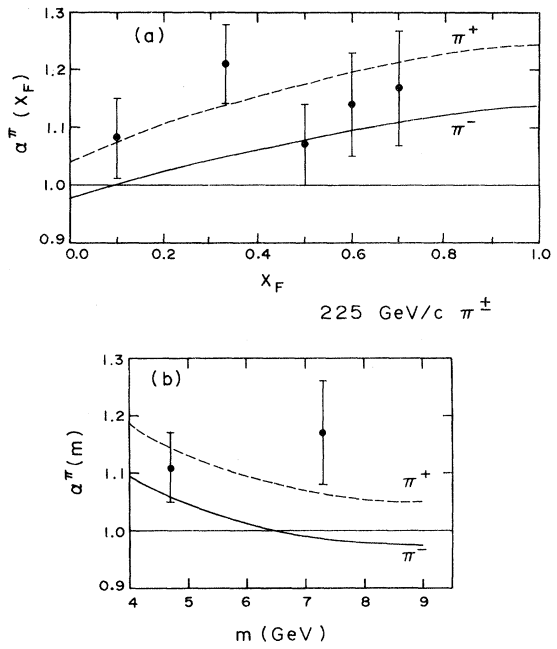

FIG. 1. Behavior of (a) $\alpha^\pi(x_F)$ and (b) $\alpha^\pi(m)$ for a pion beam of laboratory momentum 225 GeV/c impinging on copper and tungsten targets. The points are the π^- data of the CIP group (Ref. 6). The solid (dashed) curve is our calculation for the incident π^- (π^+). The straight line at $\alpha=1.0$ is drawn for reference.

2. π^+ beams

It is expected that the A dependence for π^+ beams should be stronger than for π^- beams. To see this, let us consider the simplified case in which the pion sea is neglected and the target A_0 is an isoscalar; from Eq. (12)

$$H^{\pi^+A_0}=\frac{A}{9}V^\pi(x_1)\left\{u_v^N(x_2)+5\left[S^N(x_2)+\frac{A-1}{2}\delta(1-x_2)^\mu\right]\right\}. \tag{31}$$

$$H^{\pi^-A_0}=\frac{A}{9}V^\pi(x_1)\left\{4u_v^N(x_2)+5\left[S^N(x_2)+\frac{A-1}{2}\delta(1-x_2)^\mu\right]\right\}. \tag{32}$$

where

$$u_v^N(x_2)\equiv\tfrac{1}{2}[u_v^p(x_2)+d_v^p(x_2)]. \tag{33}$$

The terms in square brackets, which are the same for π^+ and π^-, can be important only for $x_2\simeq 0$, i.e., for small dimuon masses, and decrease very rapidly for large x_2. Therefore, due to the absence of the factor 4 in the first term in Eq. (31), as compared to Eq. (32), the variation with A for a π^+ beam will be felt up to relatively large values of x_2; in other words, we expect $\alpha^{\pi^+}(m)\gtrsim\alpha^{\pi^-}(m)$.

The expected behaviors of $\alpha(x_F)$ and $\alpha(m)$ for a π^+ beam (at 225 GeV/c incident on the same pair of targets Cu and W as in the π^- case) are shown in Fig. 1. It may be mentioned that as we go to still larger values of m [not shown in Fig. 1(b)], $\alpha^{\pi^+}(m)$ will reach a plateau and increase slightly. As this interesting feature should become noticeable even earlier ($m\sim 7$ GeV) when neutron-deficient targets such as hydrogen are involved in the analysis, we shall deal with this point later when discussing the target dependence of α.

3. Proton beams

For incident protons the calculated values of $\alpha^p(x_F)$ and $\alpha^p(m)$ are presented in Fig. 2 together with the experimental data of the CFS group.[4] The data point[16] in Fig. 2(a),

$$\alpha^p_{\rm CFS}=1.007\pm0.018\pm0.028, \tag{34}$$

is an average over observations at $p_{\rm lab}=200$, 300, 400, GeV/c, each of which has a different range of acceptance of x_F values. The above point plotted at $x_F=-0.04\pm0.11$ (corresponding to the ac-

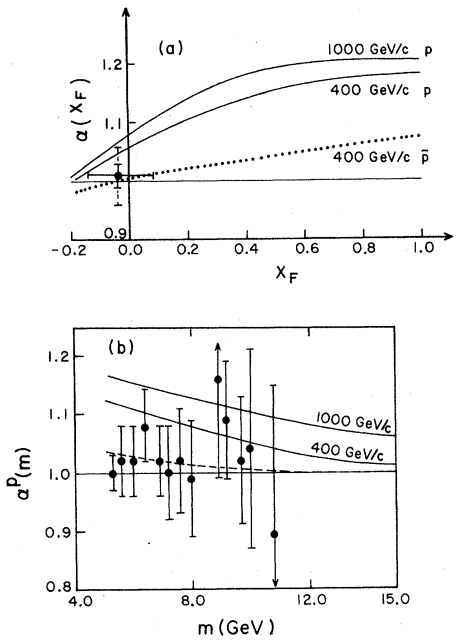

FIG. 2. Behavior of (a) $\alpha(x_F)$ and (b) $\alpha(m)$ for a proton beam for two lab momenta 400 and 1000 GeV/c incident on beryllium and platinum targets. The data points refer to the results of the CFS group (Ref. 4). In (b), the solid curves refer to integrations over the range $x_F = (0,1)$ and the dashed curve refers to the 400-GeV/c p beam with the x_F cut of the CFS group $x_F = (-0.15, +0.075)$. For comparison, the expected behavior of $\alpha(x_F)$ for a 400 GeV/c $\bar{p}$ beam is shown by the dotted line in (a); the corresponding curve in (b) is not shown as it very nearly coincides with the line $\alpha(m)=1$.

ceptance of the 400-GeV/c beam) lies slightly below the curve calculated for a 400-GeV/c p beam producing dimuons in the range $m = 5$–15 GeV. Indeed, fine-bin measurements at small values of x_F in the range implied by Eq. (28).

$$0 \lesssim x_F \lesssim \frac{2m}{\sqrt{s}}, \tag{35}$$

should reveal sizable variation in $\alpha(x_F)$ due to the steepness of the function (30). At large x_F, however, a flattening of $\alpha(x_F)$ at a value above unity is expected as in Fig. 2(a).

It is interesting to note that the additional sea which is highly peaked at small x_2 can induce different behaviors of $\alpha(x_F)$, namely, steady rise at small x_F and flattening at large x_F. This is understandable because at large x_F the values of x_2 are too small (e.g., at $x_F = 0.9$, $x_2 = 0.05$, whereas at $x_F = 0$, $x_2 \sim 0.22$) to sense any variation through the function $(1-x_2)^{\mu}$. In any case the data using large-acceptance spectrometers of the Michigan-Northeastern-Tufts-Washington (MNTW) group[17] and also of the NA3 group would, in the near future, be able to test these features of $\alpha(x_F)$.

As for the m dependence, the solid curve labeled 400 GeV in Fig. 2(b) shows the variation of $\alpha^p(m)$ when x_F is integrated over the range 0–1. Since the experimental points refer to the CFS data which have a severe cut, $-0.15 \leq x_F \leq 0.075$, we have recalculated $\alpha^p(m)$ by restricting the x_F integration to this region. The dashed line in Fig. 2(b) provides for this cut, which shows that $\alpha^p(m)$ becomes almost independent of m, as the data indicate. The values of α^p calculated with and without the x_F cut also reflect this sensitivity to the cut, as shown in Table I.

4. *Antiproton beams*

The dotted line in Fig. 2(a) shows the expected behavior of $\alpha^{\bar{p}}(x_F)$ at a laboratory momentum of 400 GeV/c. In comparison to the case of a proton beam, the effect of additional sea is weaker for a $\bar{p}$ beam of the same momentum: When $\alpha^p(x_F)$ varies from 1.05 to 1.18 in the range $x_F = 0$–1, we see that $\alpha^{\bar{p}}(x_F)$ varies only from 1.00 to 1.07. This behavior is of course not surprising as the presence of the three valence antiquarks in the beam makes the first term of $H^{\bar{p}A}$ of Eq. (12) dominate over the rest of the terms. We have also noted that the onset of saturation of $\alpha^{\bar{p}}(m)$ is at a lower dimuon mass than that of $\alpha^p(m)$; the saturated value of $\alpha^{\bar{p}}(m > 7$ GeV) is 0.99 and is not shown in Fig. 2(b). For the total cross sections at 400 GeV/c we find $\alpha^{\bar{p}} = 1.02$, which may be compared with the value $\alpha^p = 1.11$ listed in Table I. These features would be of special interest when the $\bar{p}$ beams become available at the Tevatron phase II at Fermilab.

5. *Kaon beams*

The A dependence of massive dilepton production with K^+ and K^- beams should in some sense be similar to the cases of p and $\bar{p}$ beams, respectively. The K^+ does not possess a valence $\bar{q}$ which can annihilate with the valence q of the target nucleus. This implies that in Eq. (12) the first term in H^{K^+A} is absent, while it is present in H^{K^-A}; thus the A dependence should be slightly stronger for a K^+ beam than for a K^- beam,

$$\alpha^{K^+} > \alpha^{K^-} \simeq 1. \tag{36}$$

It would be interesting to test this behavior when the $K^{\pm}$ beams of sufficient intensity and purity become available.

B. Energy dependence of α

It is interesting that the influence of a tiny additional nuclear sea can be felt increasingly at higher energies. The increase of $\alpha(x_F)$ at small x_F will be faster at higher beam momenta, and

correspondingly also the decrease of $\alpha(m)$. A comparison of these behaviors, e.g., in the case of proton beams of momenta 400 GeV/c and 1000 GeV/c, is given in Fig. 2. The corresponding value of α^p changes from 1.11 to 1.15 (see also Table II). This increase of α with the c.m. energy $\sqrt{s}$ is understandable; as $(m/\sqrt{s})$ decreases, by virtue of Eq. (29), the values of x_2 will be smaller not only at large x_F but also in the region of intermediate values of x_F, thus allowing the additional sea to contribute over a larger range of x_F integration.

The energy dependence of $\alpha(x_F)$ and $\alpha(m)$ for the case of $\pi^\pm$ beams at 200 and 400 GeV/c incident on H_2 and Pt targets are shown in Fig. 3, while the values of α corresponding to the total cross sections are given in Table II.

We note that the increase in α with beam momentum is almost entirely due to the presence of the additional sea; in the absence of the latter, for instance both at 200 GeV/c and 400 GeV/c α^{π^+} has the same value 1.01 for Cu and W targets. An observation of increasing α with beam energy thus clearly indicates the existence of the additional quark sea in the nucleus.

Table II also shows that the rate of variation of α with energy depends on the specific pairs of target nuclei employed in the experiment. This point will be elaborated upon in the following subsection.

C. Comparison of data from hydrogen target and other targets

The effect of neutron excess in the target is most pronounced when the data with heavy targets are compared with those from hydrogen target. To appreciate such a target dependence of α, we shall start by considering the case of a π^- beam on a general nuclear target A with Z protons and N neutrons; from Eq. (12)

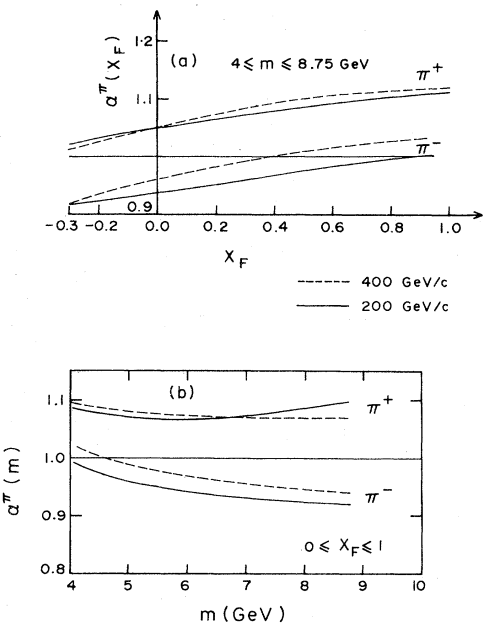

FIG. 3. Expected behaviors of (a) $\alpha^\pi(x_F)$ when integrated over the mass range 4.0 to 8.75 GeV, and (b) $\alpha^\pi(m)$ when integrated over $x_F=0$ to 1, for the $\pi^\pm$ beams incident on hydrogen and platinum targets. The solid (dashed) curves refer to 200- (400-) GeV/c pion beams.

$$H^{\pi^- A}(x_1,x_2)=\tfrac{1}{9}V^\pi(x_1)[4Zu_v^p(x_2)+4Nd_v^p(x_2)+5AS^N(x_2)+5AS_a^N(x_2)]$$
$$+\tfrac{1}{9}S^\pi(x_1)[(4Z+N)u_v^p(x_2)+(4N+Z)d_v^p(x_2)+11AS^N(x_2)+12AS_a^N(x_2)]\,, \tag{37}$$

wherein the sea functions S^N, S^π and S_a^N are defined by Eqs. (19), (24) and (30), respectively. From this we can calculate the x_2 distribution

$$\frac{d\sigma^{\pi^- A}}{dx_2}=K\frac{4\pi\alpha^2}{9sx_2^2}\int_{x_{1l}}^{x_{1u}}\frac{dx_1}{x_1^2}H^{\pi^- A}(x_1,x_2)\,, \tag{38}$$

TABLE II. Dependence of α on the nuclear targets when the integrations cover the ranges $4 \le m \le 8.75$ GeV and $0 \le x_F \le 1$.

Target pairs	(H, Pt)		(C, W)		(Cu, W)	
Beam momentum (GeV/c)	200	400	200	400	200	400
α^{π^-}	0.96	0.99	1.02	1.05	1.04	1.08
α^{π^+}	1.07	1.08	1.08	1.14	1.14	1.19
$\alpha^{\bar{p}}$	0.96	0.98	1.00	1.03	1.01	1.06
α^p	1.05	1.07	1.10	1.14	1.18	1.24

where

$$x_{1l}=\text{maximum}\left(\frac{m_l^2}{sx_2},x_2\right), \tag{39}$$

$$x_{1u}=\text{minimum}\left(1,\frac{m_u^2}{sx_2}\right), \tag{40}$$

m_l and m_u being the lower and upper cutoff values of the dimuon masses included in the data analysis. The limit (39) assumes that $x_F \ge 0$. For a pair of targets with mass numbers A_1 and A_2 we define, for $A_1<A_2$,

$$\rho_{\pi^-}(x_2)\equiv\frac{(1/A_1)(d\sigma^{\pi^- A_1}/dx_2)}{(1/A_2)(d\sigma^{\pi^- A_2}/dx_2)} \tag{41}$$

$$=\left(\frac{A_1}{A_2}\right)^{\alpha^{\pi^-}(x_2)-1}. \tag{42}$$

Thus $\alpha(x_2)$ will turn out to be less than unity if the measured ratio ρ of the normalized cross section exceeds unity (since $A_1<A_2$),

$$\alpha(x_2)=1-\frac{\ln\rho(x_2)}{\ln(A_2/A_1)}. \tag{43}$$

Before studying the exact expression for $\rho(x_2)$, it may be instructive first to note some general features by considering an approximate expression for it by neglecting all the sea distributions S's in Eq. (37). In this approximation the integral in Eq. (38) need not be evaluated, and hence

$$\rho_{\pi^-}(x_2)\simeq\frac{1-\frac{N_1}{A_1}\left(1-\frac{d_v^p(x_2)}{u_v^p(x_2)}\right)}{1-\frac{N_2}{A_2}\left(1-\frac{d_v^p(x_2)}{u_v^p(x_2)}\right)}. \tag{44}$$

The following remarks are obvious. (i) For isoscalar targets, and more generally for pairs of targets such that $(N_1/A_1)\simeq(N_2/A_2)$, $\rho\simeq1$. (ii) For other targets we envisage $\rho\neq1$ because $d_v\neq u_v$. (iii) If $u_v(x_2)=2d_v(x_2)$, one obtains a constant value

$$\rho_{\pi^-}(x_2)\simeq\frac{1+(Z_1/A_1)}{1+(Z_2/A_2)} \tag{45}$$

which exceeds unity provided $(Z_1/A_1)>(Z_2/A_2)$. The latter condition is satisfied for most of the elements since $A_1<A_2$. (iv) On the other hand, for a more realistic parametrization

$$\frac{d_v^p(x_2)}{u_v^p(x_2)}\simeq C(1-x_2);\ C\simeq0.57, \tag{46}$$

ρ increases with x_2 towards the larger value $Z_1A_2(Z_2A_1)^{-1}$. We thus observe that large values of ρ_{π^-}, which also show sizable increase with x_2, occur when the lighter target is taken to be H and the other to be a very heavy nucleus,

$$\rho_{\pi^-}(x_2)\simeq\frac{A_2}{Z_2+CN_2(1-x_2)}. \tag{47}$$

For instance, for the pair of targets employed by the NA3 group, viz. H and Pt, the right side becomes $1.35(1-0.46x_2)^{-1}$ and $\rho(x_2)>1$, or $\alpha(x_2)<1$. Thus when hydrogen-target data are included, the resulting values of $\alpha^{\pi^-}(m)$ and also $\alpha^{\pi^-}(x_F)$ are likely to lie below unity. This trend is noticeable even in the exact calculations which include the projectile- and target-sea functions, as can be seen, for example, by comparing Fig. 3(b) of H and Pt targets with Fig. 1(b) of Cu and W targets.

Turning now to the exact expression for $\rho(x_2)$ in Eq. (41), we see that the sea distributions associated with a nucleon in the target influence the values of ρ, especially at small x_2. In Fig. 4 these calculated values of $\rho(x_2)$ are given by the solid (dashed) curve when the additional nuclear sea in Eq. (37) is present (absent) for a 150-GeV/c pion beam on H and Pt targets corresponding to $4\leq m\leq8.75$ GeV and $0\leq x_F\leq1$. The preliminary data of the NA3 group[5] with π^- beam are consistent with both the solid and dashed curves in Fig. 4. Our calculated value of α^{π^-} as defined in Eq. (13) is 0.95 which implies for the ratio of x_2-integrated cross sections,

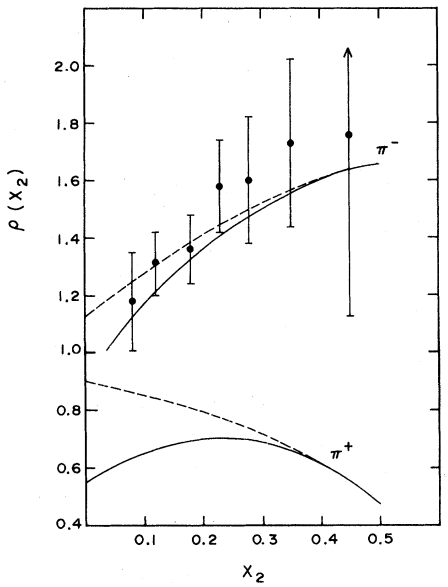

FIG. 4. The ratio of normalized cross sections $\rho(x_2)$ defined in Eq. (41) for a 150-GeV/c pion beam on hydrogen and platinum targets. The points are the preliminary data of the NA3 group (Ref. 5) for the π^- beam. The solid (dashed) curves are the expectations according to the Drell-Yan model when the additional nuclear sea is (is not) included.

$$\hat{\rho}\equiv\frac{\int dx_2(d\sigma^{\pi^-p}/dx_2)}{\frac{1}{A}\int dx_2(d\sigma^{\pi^-\mathrm{Pt}}/dx_2)}=A^{1-\alpha^{\pi^-}}, \tag{48}$$

a value 1.30, consistent with the mean value 1.4 reported by the NA3 group.[18]

The case of π^+ beams can be dealt with similarly—for instance, the analog of Eq. (44), obtained by simply replacing N_i by Z_i, instead implies $\rho_{\pi^+}(x_2)<1$ for most of the targets; when the lighter target is hydrogen we get in place of Eq. (47)

$$\rho_{\pi^+}(x_2)\simeq A_2\frac{C(1-x_2)}{Z_2C(1-x_2)+N_2}, \tag{49}$$

which decreases with x_2, causing $\alpha^{\pi^+}(x_2)$ to increase. Thus $\alpha^{\pi^+}(m)$ *will increase with* m—a trend borne out by our calculations inclusive of the sea effects—as shown by the solid curve in Fig. 3(b). The initial decrease of this curve is due to the contributions from the nuclear sea which are important at small $x_2\sim0$ (or small m) and disap-

pear elsewhere, leading to a plateau. As the effects of the additional sea are felt increasingly at higher energies, the dotted curve for 400 GeV/c shows an extended plateau region, and the upturn of $\alpha^{\pi^+}(m)$ occurs at larger values of m (not shown in the Figure). It should be noted that the different behaviors of $\alpha(m)$ with π^+ and π^- beams, which arise mainly because of Eq. (46), are quite sensitive to the targets employed; for instance, in Fig. 1(b) the $\alpha(m)$ for π^+ as seen with Cu and W targets ($Z_1/A_1 \simeq Z_2/A_2$) continues to decrease even at $m \sim 9$ GeV, while for H and Pt targets in Fig. 3(b) there is an increase.

The target dependence of α should perhaps be most striking in the case of p beams due to the absence of the valence-valence term in the Drell-Yan formula. In the expression for the function H,

$$H^{pA}(x_1,x_2)=\frac{A}{9}\Big\{S^N(x_1)\Big[\frac{4Z+N}{A}u_v^p(x_2)+\frac{4N+Z}{A}d_v^p(x_2)\Big] + [4u_v^p(x_1)+d_v^p(x_1)+\tfrac{21}{2}S^N(x_1)]S^N(x_2) + [4u_v^p(x_1)+d_v^p(x_1)+11S^N(x_2)]S_a^N(x_2)\Big\}, \tag{50}$$

the first two terms that describe the composition of the target are unimportant at large x_1 and small x_2. Therefore the ratio of cross sections (integrated over $x_F=0-1$) has the form

$$\frac{A_1[\Phi+(A_1-1)]}{A_2[\Phi+(A_2-1)]}=\left(\frac{A_1}{A_2}\right)^{\alpha^p}, \tag{51}$$

wherein, for targets other than hydrogen, it is reasonable to regard the quantity Φ as being independent of (Z_i/A_i) and (N_i/A_i). We thus expect that for a fixed A_2 ($>A_1$) α^p should increase with A_1.

This general increasing trend of α with the mass number of the target at a given beam momentum is evident in the calculated values listed in Table II. The increase of α with A_1, which is a direct consequence of the proposed additional quark sea in nuclei, is maximal for a p beam. In particular, for any given type of beam, the experiments employing H_2 as one of the targets will imply a smaller value of α than those in which both the targets are taken to be heavy.

IV. CONCLUDING REMARKS

The quark-antiquark sea in nuclei, whose consequences have been explored in the Drell-Yan processes in this paper, has its origin in the interactions of the nucleons bound in the target nucleus. This sea, which is in addition to the sea that is customarily associated with a single nucleon, is characterized by a quadratic A dependence. Such a proposal is not in conflict with any known information; the usual low-energy nuclear phenomena deal with a time-averaged picture while the hard-scattering processes involving high-momentum-transfer probes are indeed the ones which provide us with an instantaneous picture of the target. In addition, the observed anomalous nuclear enhancement in the inclusive reactions involving high-p_T hadrons and jets do seem to already suggest the existence of such a sea.

We have used the data on π^- and p collisions with nuclear targets producing massive dimuons to estimate the parameters characterizing this additional sea. Note that in the deep-inelastic scattering the contributions of the $q\bar{q}$ sea play only a minor role compared to the valence quarks of the target, and hence the eN and νN data are not suitable for an accurate determination of the sea parameters. The Drell-Yan processes in pN collisions, on the other hand, proceed dominantly with the help of the sea quarks. Secondly, in these processes (unlike in the case of the production of high p_T hadrons or jets in hadron-hadron collisions) the final $\mu^+\mu^-$ is unlikely to suffer multiple scattering within the nucleus. Thus the procedure we have adopted in estimating the typical values of the sea parameters δ and μ is reasonably clean. In any case, as the α's are defined through the ratios of cross sections, they will not be as sensitive to changes in the values of δ and μ as the individual cross sections would be.

From the definitions (13)–(15) it is evident that the functions $\alpha(x_F)$ and $\alpha(m)$ shown in Figs. 1–3 cannot be directly related to the α's given in Tables I and II; e.g., the area under the curve $\alpha(m)$ in Fig. 2(b) for a 400-GeV/c p beam is not equal to the value of α^p given in Table I.

Our calculations have obvious implications on the observed K factor in Drell-Yan processes. If the K factor were extracted naively by using the data from targets other than hydrogen, it will exhibit a dependence on the variables x_F and m since

$$K=K_{\rm QCD}A^{\alpha(x_F,m)-1}.$$

Therefore one has to first eliminate the characteristic dependences on x_F and m arising from the nuclear sea before the calculated QCD prediction[19] $K_{\rm QCD}$ is confronted with experiment.

In summary, the proposed quark-antiquark sea in nuclei gives rise to several interesting and testable consequences in regard to the A dependence in the Drell-Yan process: (i) the $\alpha(x_F)$ will increase with the Feynman variable x_F, (ii) a related feature is the general decrease of $\alpha(m)$ with the increase of the dimuon mass m (except for π^+

collisions), (iii) as the beam momentum increases the α describing the total cross section for muon-pair production will increase towards the asymptotic value 2, (iv) the α's corresponding to the positive beams p, π^+, and K^+ would be larger than the corresponding antiparticle beams, with the α for the proton beam being the largest, and (v) experiments using heavy nuclear targets would reveal a stronger A dependence than the ones which include data on hydrogen targets.

---

[1]See, for instance, the review by James E. Pilcher, in *Proceedings of the 1979 International Symposium on Lepton and Photon Interactions At High Energies, Fermilab*, edited by T. B. W. Kirk and H. D. I. Abarbanel (Fermilab, Batavia, Illinois, 1980), p. 185.

[2]S. D. Drell and T.-M. Yan, Phys. Rev. Lett. 25, 316 (1970); 25, 902(E) (1970); Ann. Phys. (N.Y.) 66, 578 (1971).

[3]J. Badier *et al.*, Phys. Lett. 89B, 145 (1979).

[4]D. F. Kaplan *et al.*, Phys. Rev. Lett. 40, 435 (1978); L. M. Lederman, in *Proceedings of the 19th International Conference on High Energy Physics, Tokyo, 1978*, edited by S. Homma, M. Kawaguchi, and H. Miyazawa (Phys. Soc. of Japan, Tokyo, 1979), p. 706.

[5]J. Badier *et al.*, CERN Report No. CERN/EP 80-150, 1980 (unpublished).

[6]K. J. Anderson *et al.*, Phys. Rev. Lett. 42, 944 (1979).

[7]K. V. L. Sarma, Phys. Rev. D 22, 216 (1980).

[8]Andre Krzywicki, Phys. Rev. D 14, 152 (1976).

[9]J. W. Cronin *et al.*, Phys. Rev. D 11, 3105 (1975); U. Becker *et al.*, Phys. Rev. Lett. 37, 1731 (1976); L. Kluberg *et al.*, *ibid.* 38, 670 (1977); D. Antreasyan *et al.*, Phys. Rev. D 19, 764 (1979).

[10]C. Bromberg *et al.*, Phys. Rev. Lett. 42, 1202 (1979); 43, 1057(E) (1979).

[11]J. H. Kühn, Phys. Rev. D 13, 2948 (1976); J. Pumplin and E. Yen, *ibid.* 11, 1812 (1975); P. V. Landshoff, J. C. Polkinghorne, and D. M. Scott, *ibid.* 12, 3738 (1975); G. R. Farrar, Phys. Lett. 56B, 185 (1975); C. O. Escobar, Phys. Rev. D 19, 844 (1979); A. Krzywicki *et al.*, Phys. Lett. 85B, 407 (1979).

[12]F. Takagi, Phys. Rev. Lett. 43, 1296 (1979); Prog. Theor. Phys. 65, 1454 (1981).

[13]J. G. H. de Groot *et al.*, Phys. Lett. 82B, 456 (1979); Z. Phys. C 1, 143 (1979).

[14]The average fraction of the longitudinal momentum carried by the valence quarks ξ_v, and that carried by the total quark sea ξ_s associated with a nucleon are given by

$$\xi_v = \int_0^1 dx[u_v^p(x) + d_v^p(x)] = 0.34 ,$$

$$\xi_s = \int_0^1 dx[5S^N(x) + 6\frac{A-1}{2}\delta(1-x)^\mu] = 0.15 + \frac{3(A-1)\delta}{\mu+1} ,$$

using Eqs. (17)–(19). For values of δ and μ in Eqs. (25) and (26), the A-dependent sea begins to be noticeable for targets heavier than Be and C ($A \gtrsim 10$); for a heavy nucleus such as platinum the momentum in the sea component, $\xi_s = 0.15 + 0.13 = 0.28$, becomes comparable to $\xi_v = 0.34$.

[15]This feature of the A dependence with regard to x_F had already been emphasized in Ref. 7.

[16]J. Lefrançois, in *High Energy Physics—1980*, proceedings of the XXth International Conference, Madison, Wisconsin, edited by L. Durand and L. G. Pondrom (AIP, New York, 1981).

[17]L. W. Jones *et al.*, in *Proceedings of the Xth International Symposium on Multiparticle Dynamics, Goa, India, 1979*, edited by S. N. Ganguli, P. K. Malhotra, and A. Subramanian (Tata Institute of Fundamental Research, Bombay, India, 1979), p. 675.

[18]It should be emphasized that our definition of α in Eq. (48) is quite different from the one used by the NA3 collaboration (Ref. 5):

$$\hat{\rho}(\text{observed}) = A^{1-\alpha_{NA3}}\hat{\rho}(\text{DY}) ,$$

where $\hat{\rho}$(DY) is calculated from the standard Drell-Yan formula (assuming the K factor to be A independent) to be 1.39. According to our definition the left side of Eq. (48) is calculable by including the effects of the nuclear sea. Therefore we should have, by comparing the two definitions,

$$\alpha_{NA3} = \alpha + \frac{\ln\hat{\rho}(\text{DY})}{\ln A} = 1.01 ,$$

which is in accord with the preliminary value of the NA3 group 0.994 ± 0.015 obtained by ignoring the pion sea.

[19]J. Kubar-Andre and F. E. Paige, Phys. Rev. D 19, 221 (1979); G. Altarelli, R. K. Ellis, and G. Martinelli, Nucl. Phys. B157, 461 (1979); K. Harada, T. Kaneko, and N. Sakai, *ibid.* B155, 169 (1979); J. Abad and B. Humpert, Phys. Lett. 80B, 286 (1979); B. Humpert and W. L. Van Neerven, *ibid.* 89B, 69 (1979); J. Kubar *et al.*, Nucl. Phys. B175, 251 (1980).